frontiers in Energy Research

ORIGINAL RESEARCH
published: 07 March 2022
doi: 10.3389/fenrg.2022.846752

Effects of Stepwise Microwave Synergistic Process Water Recirculation During Hydrothermal Carbonization on Properties of Wheat Straw

Xinyan Zhang[1], Qingyu Qin[2], Xian Liu[2] and Wenlong Wang[1]**

[1]National Engineering Laboratory for Reducing Emissions from Coal Combustion, Shandong Key Laboratory of Energy Carbon Reduction and Resource Utilization, Engineering Research Center of Environmental Thermal Technology of Ministry of Education, School of Energy and Power Engineering, Shandong University, Jinan, China, [2]Laboratory of Biomass and Bioprocessing Engineering, College of Engineering, China Agricultural University, Beijing, China

OPEN ACCESS

Edited by:
Hui Shang,
China University of Petroleum, Beijing, China

Reviewed by:
Cuiping Wang,
Shandong University of Science and Technology, China
Wenchao Ma,
Hainan University, China

***Correspondence:**
Xinyan Zhang
sddxzxy2020@sdu.edu.cn
Wenlong Wang
wwenlong@sdu.edu.cn

Specialty section:
This article was submitted to Process and Energy Systems Engineering, a section of the journal Frontiers in Energy Research

Received: 31 December 2021
Accepted: 24 January 2022
Published: 07 March 2022

Citation:
Zhang X, Qin Q, Liu X and Wang W (2022) Effects of Stepwise Microwave Synergistic Process Water Recirculation During Hydrothermal Carbonization on Properties of Wheat Straw. Front. Energy Res. 10:846752. doi: 10.3389/fenrg.2022.846752

In this study, wheat straw (WS) was treated using two-step synergistic techniques, which were process water recirculation (PWR) during hydrothermal carbonization (HTC) and microwave energy activation (MEA). The physicochemical properties of solid and liquid products during the process of HTC PWR were characterized. The temperature-rising properties, yields, and fuel properties of hydrochar after MEA were explored. Then the optimal technique conditions were explored. When HTC PWR was twice, the carbon content (55.59%) and higher heating value (21.72 MJ/kg) were the highest, and the ash content (1.93%) and the O/C and H/C ratios were the lowest. When HTC PWR was three times, the fixed carbon content, mass yield, and energy yield were the highest: 18.53%, 58.25%, and 71.84%, respectively. Many more carbon microspheres and pores appeared on the surface of hydrochar after PWR, which could improve the fuel characteristics and mass yield. After HTC PWR, the concentration of organic acids and HMF in liquid by-products increased, which was conducive to the increase of carbon content and mass yield. The best effect was HTC PWR twice or three times. With the increase of microwave power or the extension of microwave activation duration, the temperature-rising properties of hydrochar significantly increased, and the mass and energy yields decreased. The volatile contents of hydrochar decreased and their fixed carbon contents and HHV increased with the increase of microwave power. The properties of hydrochar could be improved when MEA was 900 W or 1000 W for 4 min. Therefore, MEA had significant effects on the properties of hydrochar after different PWR conditions.

Keywords: wheat straw, hydrothermal carbonization, process water recirculation, microwave energy activation, physicochemical property, temperature rising property

1 INTRODUCTION

Straw is a kind of abundant biomass resource, containing micronutrients, nutrient elements, and organic carbon (Cui et al., 2018). In China, the output of straw is ~900 million tons every year (Hu et al., 2021). After grain harvest, a large number of straws are stacked in the fields or burned directly, which will cause serious waste of resources and environmental pollution (Ma et al., 2019). The straws should be disposed of in some reasonable ways converting them into efficient energy resource material. Thermochemical conversion has the characteristic of a high conversion rate (Leng et al., 2020). Hydrothermal carbonization (HTC) can produce a carbon source which is an effective thermochemical conversion process (Stemann et al., 2013a; Ghaziaskar et al., 2019). It is a mild temperature (180–260°C) and pressure (~2–6 MP) reaction in an aqueous solution, converting lignocellulosic biomass into high energy density solid fuel (Funke and Ziegler, 2010; Reza et al., 2013; Libra et al., 2014; Uddin et al., 2014). However, many degradation products and inorganic biomass substances will dissolve into byproduct liquid during HTC, which causes energy loss and additional investment of wastewater treatment (Weiner et al., 2014; Kabadayi Catalkopru et al., 2017; Lenga et al., 2020). The continuous use of freshwater will cause a waste of water resources. All these problems restrict the application of the HTC technique. Therefore, it is necessary to adopt reasonable ways of process water disposal to improve the economic and environmental benefits of this technique (Weiner et al., 2014; Wang et al., 2019).

Process water recirculation (PWR) is a method that can solve the problems of water resource waste and sewage treatment, as well as reduce heat consumption (Zhu et al., 2015). PWR can also reduce the cost of wastewater treatment. The process water of HTC is rich in a variety of organic chemical compounds. These substances can catalyze dehydration and decarboxylation reactions, which can significantly improve the overall efficiency of the HTC system (Kambo et al., 2018). Studies have shown that the contents of short-chain organic acids increase with the increase of PWR numbers, which can promote the decomposition of raw materials to produce hydrochar (Köchermann et al., 2018). Stemann et al. (2013b) has found that PWR was the most effective heat recovery method during the HTC process, which can reduce a lot of external heat consumption. And process water also contributed to the anaerobic digestion of some biomass (Wirth and Mumme, 2013). Heidari et al. (2018) set different HTC conditions to explore the effects of PWR on product characteristics. The results show that when PWR is the first time, the mass yield of hydrochar increases by 12%, and its higher heating value (HHV) increases by 2%. When PWR is twice, the energy recovery efficiency increases by 15.83%. The PWR has a specific catalytic efficiency on the HTC process of biomass (Ghaziaskar et al., 2019). After PWR, the hydrophobicity of hydrochar is enhanced (Stemann et al., 2013b), and their carbon content and energy yield increase by 84% and 82%, respectively.

The microwave energy activation (MEA) technique has the characteristics of selectivity, rapidity, and integrity (Kambo, 2014). The material can be activated rapidly and directionally, thus reducing the processing time and cost. Microwave energy activation can induce local hot spots, which can specifically improve the characteristics of biomass (Zhang and Zhang, 2017; Ao et al., 2018). The study has shown that the absorption property of hydrochar is better than that of raw biomass (Zhou et al., 2020). Therefore, the combination of HTC and MEA might be a coupling treatment technique with great potential to improve straw performance.

However, the effects of HTC PWR combined with MEA on the properties of wheat straw (WS) have been sparsely reported. In this study, the WS was used as raw material. After HTC, the liquid was used for recycling in the next HTC treatment. The PWR was six times. The mass and energy yields, ultimate and proximate analyses, O/C and H/C ratios, HHV, the surface microstructure of hydrochar, and the organic chemical compounds in liquid by-products were explored. After that, the selected hydrochar was activated by microwave energy treatment. The temperature-rising properties and fuel properties of WS hydrochar were measured.

2 MATERIALS AND METHODS

2.1 Experimental Material

The methods in which WS was collected and selected were similar to the previous study (Zhang et al., 2018; Zhang et al., 2020). During the process of collection, the WS was cut at ground level. After removing the root and grain, they were machine-cut to lengths of 30–35 cm. The WS was crushed with a Retsch SM 300 pulverizer (Haan, Germany) sifted to obtain a 2 mm size, and stored in a zip-lock bag.

2.2 Process Water Recirculation During Hydrothermal Carbonization

A Parr 4848 autoclave reaction kettle (Parr Instrument Co., Moline, 1L, United States) was used for the HTC experiment of WS powder. The operation method was optimized on the basis of previous research (Zhang et al., 2020). In the HTC PWR experiment, the WS (25 g) and distilled water (375 g) were loaded into the reaction kettle in the first experiment (i.e., 0 cycle). The HTC conditions were 231°C and 25 min (Zhang et al., 2020). After every HTC experiment, the liquid by-products (~300 g) were collected for the next HTC experiment. Then distilled water (~75 g) was added into the collected liquid so that the total liquid mass was 375 g and the ratio of material to liquid is 1:15. Then the HTC experiment was carried out again based on the above operation method. A schematic diagram of PWR during HTC is shown in **Figure 1**. The HTC PWR experiment was completed six times. The liquid by-products were collected after each recirculated experiment, which was used for subsequent determination. In each group of HTC PWR experiment, the first experiment was PWR for zero time (marked as HTC-PWR0), the second experiment was PWR for the first time (marked as HTC-PWR1), and according to this naming

FIGURE 1 | Schematic diagram of process water recirculation during hydrothermal carbonization.

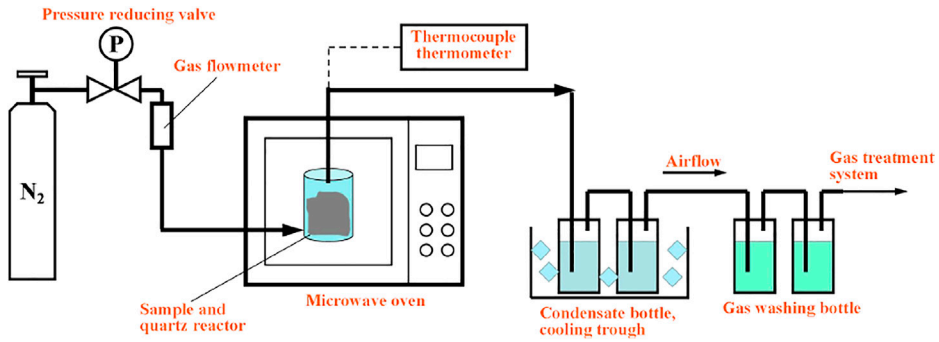

FIGURE 2 | Schematic diagram of microwave energy activation system.

method, the seventh experiment was PWR for the sixth times (marked as HTC-PWR6).

2.3 Hydrochar Characteristics

Mass yield (%) was calculated by dividing the mass of hydrochar by the mass of raw WS, both on a dry mass basis.

$$\text{mass yield}\,(\%) = \frac{\text{mass of hydrochar}}{\text{mass of wheat straw}} \times 100 \quad (1)$$

The energy densification was determined by the ratio of HHV of hydrochar and WS.

$$\text{energy densification} = \frac{\text{HHV of hydrochar}}{\text{HHV of wheat straw}} \quad (2)$$

Energy yield was calculated by a product of mass yield and energy densification (Ghaziaskar et al., 2019).

$$\text{energy yield} = \text{energy densification} \times \text{mass yield} \quad (3)$$

Elemental analyses were determined by an Elementar Vario MACRO cube (Langenselbold, Germany) (Zhang et al., 2020). The carbon, hydrogen, and nitrogen contents were determined referencing the ASTM D5373-16, and the sulfur content was determined referencing the ASTM E775. The oxygen content was calculated by the subtraction method as follows (Telmo et al., 2010; Li et al., 2018):

$$O\% = 100\% - (C\% + N\% + H\% + S\%) - ash\% \quad (4)$$

Where *C, H, N, O,* and *S* represent the carbon, hydrogen, nitrogen, oxygen, and sulfur contents, respectively, in mass percentages on a dry basis.

The proximate analyses (including ash, volatile matter, fixed carbon) were measured according to ASTM D7582-10.

The HHV was analyzed via a Parr 6300 bomb calorimeter. The analysis method was referred to ASTM E711, Channiwala and Parikh (2002) and Poddar et al. (2014). The 0.7 g sample was weighed by an electronic balance and placed on lens paper. Then the sample was wrapped put into the cube of a bomb calorimeter. The calorific value (GVC) of the cartridge was recorded after the instrument measurement. The sulfur content was determined according to the method of elemental analysis. The HHV was calculated as follows:

$$HHV\,(J/g) = GCV \times 10^3\,(J/g) - 94.2833S\,(\%) \quad (5)$$

The surface microstructure of hydrochar was analyzed by scanning electron microscope (SEM) (Japanese Electronics, Japan), a method similar to the previous research (Zhang

TABLE 1 | The mass and energy yields of wheat straw hydrochar after process water recirculation.

Sample	Mass yield (%)	Energy yield (%)
HTC-PWR0 hydrochar	50.69 ± 0.51^{b}	61.12 ± 0.29^{g}
HTC-PWR1 hydrochar	52.22 ± 0.47^{ab}	63.39 ± 0.58^{f}
HTC-PWR2 hydrochar	56.36 ± 0.56^{ab}	70.19 ± 0.65^{e}
HTC-PWR3 hydrochar	58.25 ± 0.57^{a}	71.84 ± 0.58^{a}
HTC-PWR4 hydrochar	57.90 ± 0.54^{a}	70.98 ± 0.34^{c}
HTC-PWR5 hydrochar	57.79 ± 0.07^{a}	71.31 ± 0.41^{b}
HTC-PWR6 hydrochar	57.12 ± 0.81^{a}	70.25 ± 0.66^{d}

The figures are the mean value ±standard deviation in the table.
a, b, c, d, e, f, g means followed by different superscripts in the same column are significantly different at $p < 0.05$.
a, b, c, d, e, f, g means followed by the same superscripts in the same column are not significantly different at $p > 0.05$.

et al., 2018). Before analysis, the samples were sputter-coated with gold (Kaliyan and Morey, 2010; Liu et al., 2017).

2.4 Liquid By-Product Characteristics

The concentration of organic acids, 5-Hydroxyl Methyl Furfural (HMF), and furfurals in the liquid by-product were measured using High-Performance Liquid Chromatography (HPLC) (Hitachi, Ltd., Tokyo, Japan) (Sluiter et al., 2006). The instrument and organic compounds were calibrated before the experiment. Firstly, the liquid by-product went through a 0.45 μm filter membrane. Secondly, the pH of the liquid by-product was adjusted to 2–4 using concentrated phosphoric acid. Biorad Aminex HPX-87H column was selected for HPLC analysis. The analysis conditions were: sample quantity (20 μL), mobile phase (0.1% phosphoric acid solution), flow rate (1 ml/min), column temperature (60°C). The detector temperature was close to the column temperature. UV wavelength was 210 nm.

2.5 Microwave Energy Activation

The MEA experiment was carried out in the modified microwave oven, in which a thermocouple could be used for temperature measurement. Hydrochar (20 g) was placed in a custom quartz reactor, which was placed in the geometric center of the microwave oven for activation based on the set microwave power and time. The microwave power was set to 800, 900, and 1000 W, and the microwave activation duration was set to 2, 4, and 6 min. After microwave activation, the thermocouple was quickly inserted into the sample to measure the temperature. The schematic diagram of the MEA system was shown in **Figure 2**. And then the yields, proximate analysis, and HHV of these samples were determined. The microwave energy activation conditions are denoted as MEA A-B in the manuscript and tables, where A is the microwave power (W) and B is the duration (min).

2.6 Theoretical Calculations

Microsoft Excel 2010 (Microsoft Corp., Redmond, WA, United States) was used to calculate the parameters. Origin 8.6 (Origin Lab Corp., Northampton, MA, United States) was used for plotting figures. The Statistical Package for the Social Science (SPSS) software v. 20.0 (IBM Corp., Chicago, IL, United States) was used to perform the statistical analyses. The data were analyzed by ANOVA, followed by Duncan's multiple range test. Differences among means at $p < 0.05$ were considered statistically significant.

3 RESULTS AND DISCUSSION

3.1 Effects of Process Water Recirculation on the Physicochemical Properties of Solid and Liquid Products During Wheat Straw Hydrothermal Carbonization

3.1.1 Mass Yield and Energy Yield

The mass and energy yields of hydrochar during HTC PWR are illustrated in **Table 1**. With the increase of PWR number, the mass yield of WS hydrochar increased rapidly and then decreased slightly. The mass yield (58.25%) of hydrochar was the highest in the condition of HTC-PWR3, which increased by 14.91% compared with that in HTC-PWR0. The result was higher than the results of Uddin et al. (2014). Research has shown that the cellulose and hemicellulose in biomass decomposed into soluble sugar, and the lignin degraded into aromatic alcohol in the process of HTC (de Caprariis et al., 2021; Tai et al., 2021). During PWR, these decomposition products were condensed and polymerized, then deposited on the surface of hydrochar, which led to the increase of mass yield of hydrochar (Titirici and Antonietti, 2010). After HTC-PWR3, the mass yield change

TABLE 2 | The ultimate and proximate analyses of wheat straw hydrochar after process water recirculation.

Sample	Ultimate analysis (w.t. %)					Proximate analysis (w.t. %)		
	C	H	N	S	O	Ash	Volatile	Fixed carbon
HTC-PWR0 hydrochar	51.92 ± 0.19^{c}	6.50 ± 0.03^{a}	0.51 ± 0.02^{c}	0.71 ± 0.01^{b}	38.25 ± 0.11^{a}	2.11 ± 0.11^{c}	78.63 ± 0.39^{a}	17.04 ± 0.17^{b}
HTC-PWR1 hydrochar	53.75 ± 0.16^{b}	5.36 ± 0.16^{d}	0.83 ± 0.04^{b}	1.08 ± 0.36^{a}	36.84 ± 0.16^{b}	2.15 ± 0.07^{cd}	78.29 ± 0.84^{a}	17.22 ± 0.78^{b}
HTC-PWR2 hydrochar	55.59 ± 0.77^{a}	5.61 ± 0.16^{bc}	0.92 ± 0.05^{a}	0.63 ± 0.06^{bc}	35.32 ± 0.22^{c}	1.93 ± 0.09^{e}	77.32 ± 0.14^{b}	18.22 ± 0.11^{a}
HTC-PWR3 hydrochar	54.55 ± 0.56^{b}	5.47 ± 0.13^{cd}	0.90 ± 0.03^{a}	0.51 ± 0.03^{bcd}	36.32 ± 0.18^{b}	2.26 ± 0.13^{b}	76.75 ± 0.48^{b}	18.53 ± 0.49^{a}
HTC-PWR4 hydrochar	54.44 ± 0.47^{b}	5.46 ± 0.11^{cd}	0.88 ± 0.04^{a}	0.43 ± 0.02^{cd}	36.53 ± 0.13^{b}	2.26 ± 0.01^{b}	76.95 ± 0.28^{b}	18.26 ± 0.34^{a}
HTC-PWR5 hydrochar	54.25 ± 0.34^{b}	5.44 ± 0.05^{cd}	0.91 ± 0.01^{a}	0.38 ± 0.01^{d}	36.57 ± 0.10^{b}	2.45 ± 0.07^{a}	77.11 ± 0.07^{b}	17.91 ± 0.01^{a}
HTC-PWR6 hydrochar	54.51 ± 0.08^{b}	5.55 ± 0.06^{bcd}	0.90 ± 0.01^{a}	0.36 ± 0.01^{d}	36.28 ± 0.04^{b}	2.39 ± 0.05^{a}	76.90 ± 0.11^{b}	18.15 ± 0.15^{a}

The figures are the mean value ±standard deviation in the table.
a, b, c, d, e, means followed by different superscripts in the same column are significantly different at $p < 0.05$.
a, b, c, d, e, means followed by the same superscripts in the same column are not significantly different at $p > 0.05$.

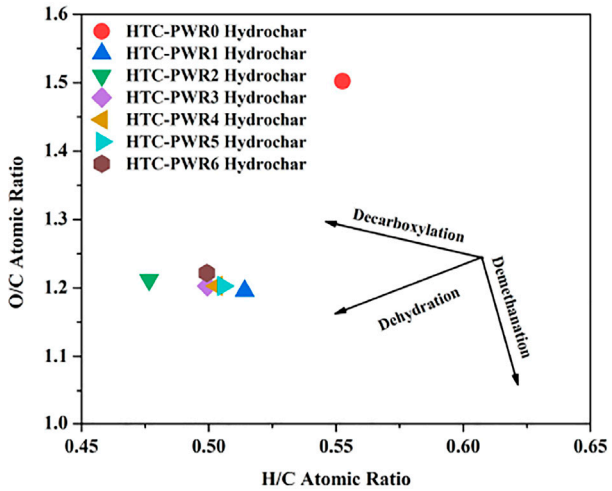

FIGURE 3 | Van Krevelen diagram of wheat straw hydrochar after process water recirculation.

was not obvious, which was because the reactions reached relative equilibrium (Stemann et al., 2013b). The results showed that the mass yield of hydrochar could be improved during the process of HTC PWR.

With the increase of PWR number, the energy yield of hydrochar first increased significantly ($p < 0.05$) and then reached a stable state. The energy yield (71.84%) was the highest after HTC-PWR3, which was 17.54% higher than that after HTC-PWR0. Therefore, the energy yield of WS hydrochar could be significantly improved after HTC PWR.

3.1.2 Ultimate and Proximate Analyses

The ultimate and proximate analyses of WS hydrochar after HTC PWR are summarized in **Table 2**. The carbon content of WS hydrochar increased after PWR. The carbon content was the highest after HTC-PWR2, which was 55.59%. With the increase of the number of PWR, the sulfur content decreased. The ash content during HTC-PWR2 was the lowest, reaching 1.93. However, the ash contents of hydrochar under the other conditions (except HTC-PWR2) were higher than that of hydrochar under HTC-PWR0, which was caused by the deposition of inorganic elements (Kambo et al., 2018). The effect of HTC PWR on the volatile content was not significant ($p > 0.05$), and their contents fluctuated within a specific range. The fixed carbon contents of hydrochar after HTC-PWR1-6 were higher than that of the hydrochar after HTC-PWR0. The fixed carbon content of hydrochar of HTC-PWR3 was the highest (18.53%), followed by those of HTC-PWR4 and HTC-PWR2.

The oxygen-to-carbon (O/C) and hydrogen-to-carbon (H/C) atomic ratios of WS hydrochar after PWR are depicted in the form of a van Krevelen diagram (**Figure 3**). Arrows in **Figure 3** represent the change in the oxygen and hydrogen contents by the dehydration and decarboxylation reactions. The O/C and H/C ratios of HTC-PWR0 hydrochar were the highest. The O/C and H/C ratios of HTC-PWR2 hydrochar were the lowest (**Figure 3**). During the process of HTC, the dehydration and decarboxylation reactions caused the oxygen and hydrogen contents to decrease, and then the carbon content relatively increased. Solid fuels have coal-like properties and are more beneficial to combustion when their O/C and H/C ratios are lower because they can reduce

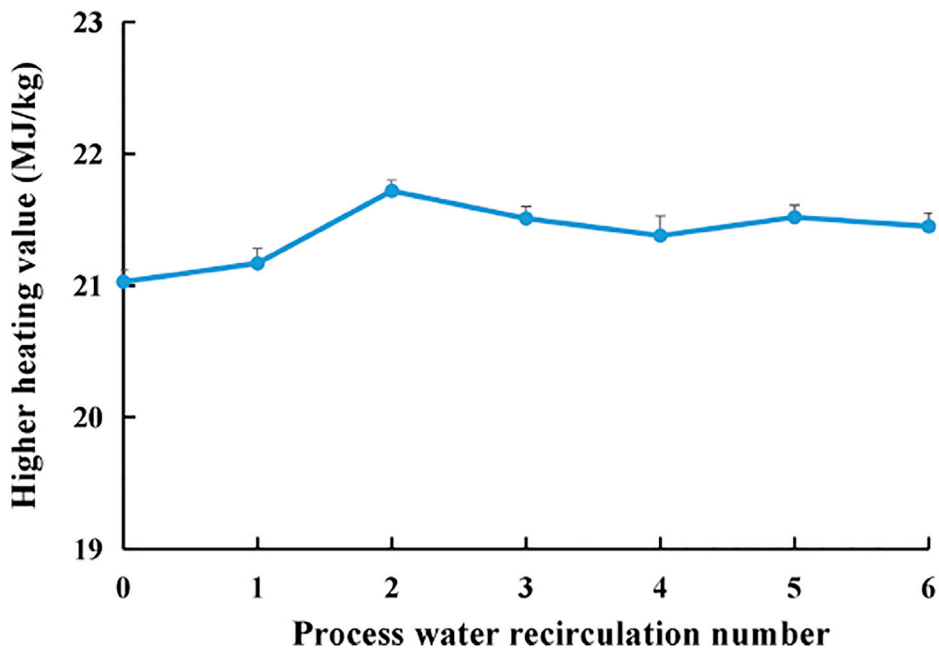

FIGURE 4 | Effects of process water recirculation on HHV of wheat straw hydrochar.

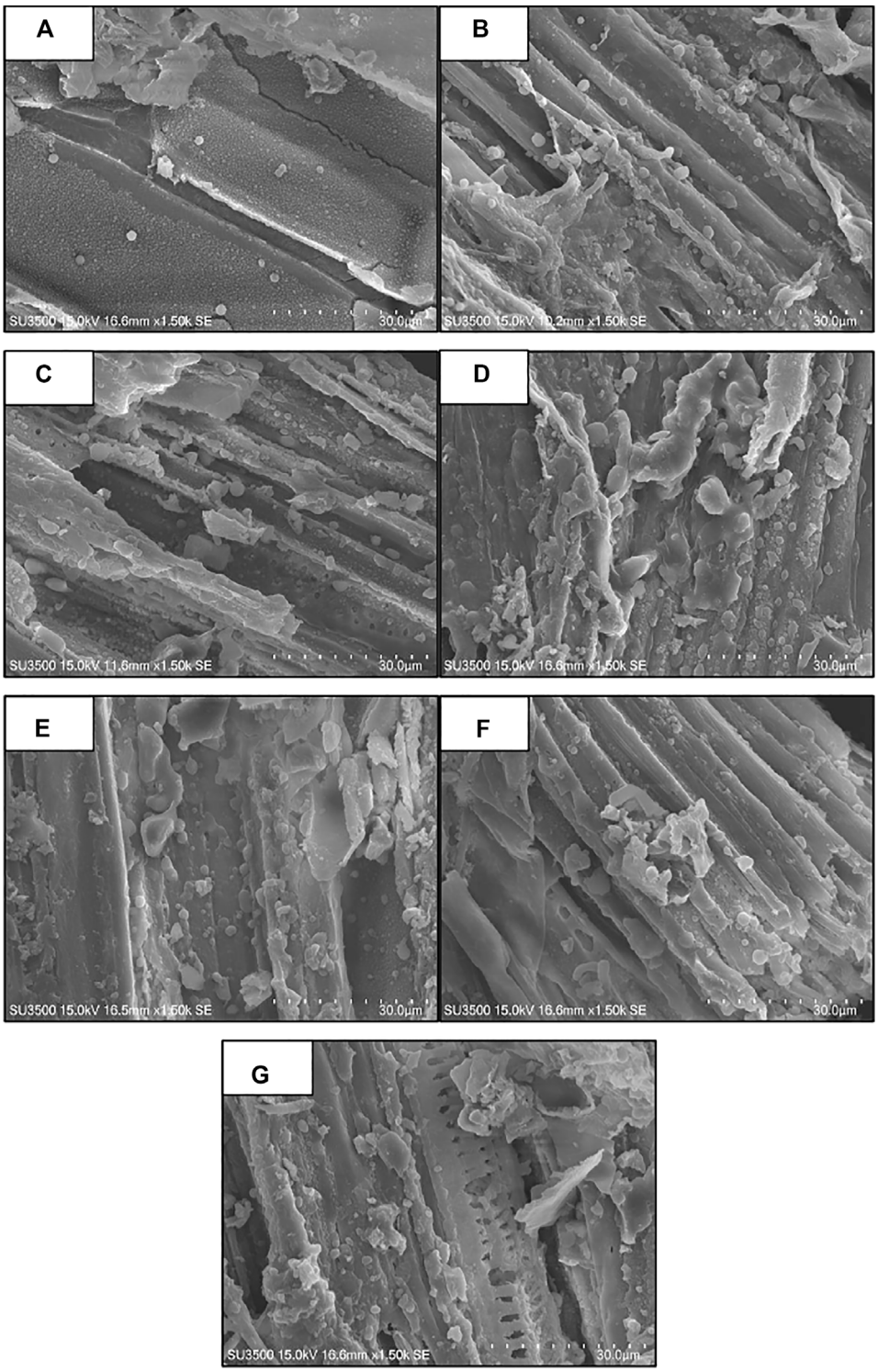

FIGURE 5 | Contrast analysis diagrams of surface microstructures of wheat straw and hydrochar [**(A)** HTC-PWR0 hydrochar, **(B)** HTC-PWR1 hydrochar, **(C)** HTC-PWR2 hydrochar, **(D)** HTC-PWR3 hydrochar, **(E)** HTC-PWR4 hydrochar, **(F)** HTC-PWR5 hydrochar, **(G)** HTC-PWR6 hydrochar].

TABLE 3 | Organic chemical compounds of liquid by-products after hydrothermal carbonization process water recirculation.

Process water recirculation number	Organic acids					Intermediate product	
	Acetic acid (mg/ml)	Glycolic acid (mg/ml)	Levulinic acid (mg/ml)	Formic acid (mg/ml)	Lactic acid (mg/ml)	HMF (mg/ml)	Furfurals (mg/ml)
0	1.35 ± 0.01^{f}	0.41 ± 0.02^{f}	1.09 ± 0.03^{f}	1.79 ± 0.01^{f}	2.21 ± 0.01^{e}	2.33 ± 0.03^{g}	1.05 ± 0.05^{f}
1	1.56 ± 0.01^{e}	0.53 ± 0.01^{e}	1.11 ± 0.01^{e}	1.94 ± 0.01^{e}	2.52 ± 0.01^{d}	2.40 ± 0.01^{f}	1.21 ± 0.01^{e}
2	3.59 ± 0.12^{c}	1.68 ± 0.01^{c}	1.18 ± 0.01^{d}	2.44 ± 0.04^{c}	5.17 ± 0.08^{b}	4.10 ± 0.01^{c}	2.09 ± 0.01^{b}
3	3.62 ± 0.03^{c}	1.64 ± 0.02^{c}	1.19 ± 0.01^{c}	2.43 ± 0.01^{c}	5.18 ± 0.02^{b}	6.04 ± 0.01^{a}	3.99 ± 0.01^{a}
4	5.00 ± 0.04^{b}	2.42 ± 0.02^{b}	1.20 ± 0.01^{a}	2.98 ± 0.02^{b}	6.39 ± 0.01^{a}	4.23 ± 0.01^{b}	1.87 ± 0.03^{c}
5	5.36 ± 0.01^{d}	2.45 ± 0.01^{d}	1.25 ± 0.01^{c}	2.94 ± 0.01^{d}	7.23 ± 0.01^{c}	2.52 ± 0.01^{e}	1.47 ± 0.01^{d}
6	5.54 ± 0.03^{a}	2.67 ± 0.01^{a}	1.27 ± 0.01^{b}	3.05 ± 0.02^{a}	7.30 ± 0.02^{a}	3.59 ± 0.01^{d}	2.05 ± 0.01^{b}

The figures are the mean value ±standard deviation in the table.

a, b, c, d, e, f, means followed by different superscripts in the same column are significantly different at $p < 0.05$.

a, b, c, d, e, f, means followed by the same superscripts in the same column are not significantly different at $p > 0.05$.

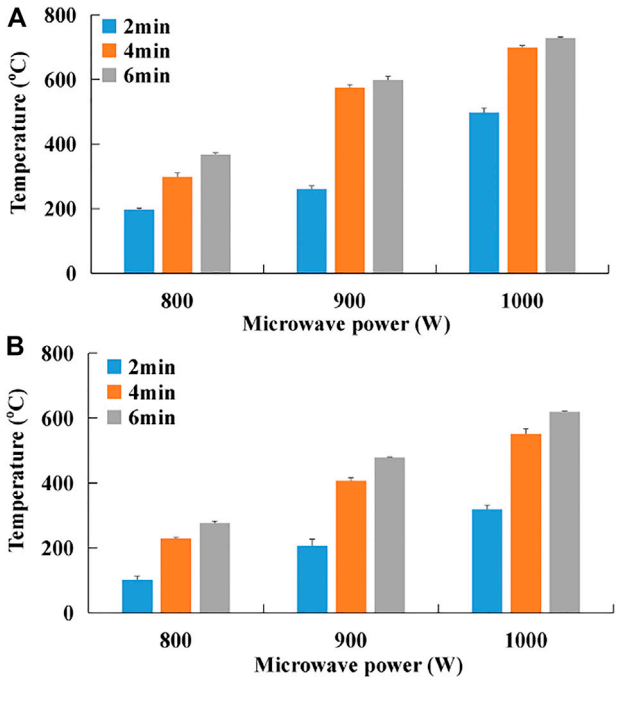

FIGURE 6 | Effects of microwave energy activation on temperature-rising property of wheat straw hydrochar [**(A)** HTC-PWR2 hydrochar; **(B)** HTC-PWR3 hydrochar].

smoke, water vapor, and energy loss during combustion (Liu et al., 2013). Therefore, HTC-PWR2 hydrochar had the potential to become a high-value fuel.

3.1.3 Higher Heating Value

The variations in HHV of hydrochar in the process of HTC PWR are reported in **Figure 4**. As shown in **Figure 4**, the HHV first went up, and then it had a small reduction before reaching a steady state. The HHV (21.72 MJ/kg) of HTC-PWR2 hydrochar was the highest. These results were due to the degradation of cellulose, hemicellulose, and lignin during the process of HTC PWR, producing HMF with a high-energy bond. Meanwhile, the dehydration and decarboxylation reactions could increase the carbon content. These factors together caused the rise in HHV (Ghaziaskar et al., 2019). However, with the increase of PWR number, the HMF rehydrated to the compounds with low calorific value, such as levulinic acid and formic acid, which led to a decrease of HHV (Salak Asghari and Yoshida, 2006).

3.1.4 Surface Microstructures

The comparative analysis diagrams of the surface microstructure of WS and its hydrochar were analyzed in **Figure 5**. The surface of HTC-PWR0 hydrochar was uneven with specific pores, and there were many carbon microspheres on the surface. With the increase of PWR number, the amounts of carbon microspheres increased. The formation of carbon microspheres could increase the carbon content of hydrochar (Ma et al., 2018; Zhang et al., 2019; Zhu et al., 2019). Starting from HTC-PWR2, the carbon microspheres began to melt. The changes in the number of carbon microspheres were consistent with the changes in the carbon content in **Table 2**, which was helpful to improve the fuel characteristics of WS hydrochar. More pores appeared on the surface of hydrochar with the increase of PWR number, which led to the small molecular compounds produced in HTC reaction being more likely to be deposited on hydrochar, thus increasing the mass yield of hydrochar (Reza, 2011; Reza et al., 2013; Uddin et al., 2014).

3.1.5 Characteristics of Liquid By-Products

The organic chemical compounds in liquid by-products during the process of HTC PWR were reported in **Table 3**. In this experiment, formic acid, acetic acid, and lactic acid in liquid by-products were organic acids with relatively high concentrations. These were due to the fact that acetic acid and formic acid were considered the stable final products in the liquid by-products during the HTC process (Jin et al., 2005). Simultaneously, the organic acids were stable in acidic high-temperature reactions and only dissolved in a liquid (Knežević et al., 2009), which accumulated with the increase of PWR number. As shown in **Table 3**, with the rise in the number of HTC PWR, the concentration of all kinds of organic acids increased. The increase of organic acids could catalyze the dehydration and decarboxylation reactions during the HTC PWR process, which was conducive to the rise of the carbon content of hydrochar and the improvement of HHV (Funke and Ziegler, 2010; Ibbett et al., 2011).

TABLE 4 | The mass and energy yields of wheat straw hydrochar after microwave energy activation.

Sample	Mass yield (%)		Energy yield (%)	
	HTC-PWR2 hydrochar	HTC-PWR3 hydrochar	HTC-PWR2 hydrochar	HTC-PWR3 hydrochar
MEA800-4	39.39 ± 0.21^{a}	38.21 ± 0.19^{a}	45.40 ± 1.35^{b}	42.39 ± 1.22^{a}
MEA900-4	37.91 ± 0.32^{c}	36.57 ± 0.21^{c}	46.18 ± 0.99^{a}	42.88 ± 0.39^{a}
MEA1000-4	35.81 ± 0.19^{e}	33.98 ± 0.21^{e}	44.02 ± 1.78^{c}	41.46 ± 0.51^{b}
MEA900-2	38.05 ± 0.57^{b}	37.16 ± 0.67^{b}	44.44 ± 2.01^{c}	41.90 ± 0.76^{b}
MEA900-6	36.57 ± 0.99^{d}	35.01 ± 0.39^{d}	42.80 ± 0.19^{d}	40.69 ± 0.89^{c}

The figures are the mean value ±standard deviation in the table.

a, b, c, d, e, means followed by different superscripts in the same column are significantly different at $p < 0.05$.

a, b, c, d, e, means followed by the same superscripts in the same column are not significantly different at $p > 0.05$.

TABLE 5 | The proximate analysis and higher heating value of wheat straw hydrochar after microwave energy activation.

Sample	Proximate analysis (w.t. %)						Higher heating value (MJ/kg)	
	Ash		Volatile		Fixed carbon		HTC-PWR2 hydrochar	HTC-PWR3 hydrochar
	HTC-PWR2 hydrochar	HTC-PWR3 hydrochar	HTC-PWR2 hydrochar	HTC-PWR3 hydrochar	HTC-PWR2 hydrochar	HTC-PWR3 hydrochar		
MEA800-4	3.12 ± 0.07^{c}	4.89 ± 0.21^{a}	75.99 ± 0.66^{d}	75.01 ± 0.75^{d}	19.78 ± 0.99^{d}	18.20 ± 1.22^{d}	22.66 ± 1.12^{d}	21.81 ± 0.22^{e}
MEA900-4	2.69 ± 0.11^{a}	5.17 ± 0.15^{d}	72.36 ± 0.91^{b}	72.17 ± 1.12^{b}	23.95 ± 0.65^{b}	21.67 ± 1.27^{b}	23.95 ± 0.78^{b}	23.05 ± 0.65^{b}
MEA1000-4	3.01 ± 0.09^{b}	5.07 ± 0.09^{c}	70.19 ± 1.22^{a}	70.55 ± 1.69^{a}	25.96 ± 1.19^{a}	23.27 ± 0.66^{a}	24.17 ± 0.33^{a}	23.99 ± 0.98^{a}
MEA900-2	3.25 ± 0.15^{d}	4.97 ± 0.06^{b}	76.21 ± 0.71^{e}	77.12 ± 0.77^{e}	19.33 ± 0.96^{d}	16.90 ± 1.58^{e}	22.96 ± 1.96^{d}	22.17 ± 0.19^{d}
MEA900-6	3.19 ± 0.21^{c}	5.51 ± 0.22^{e}	75.16 ± 1.11^{c}	74.33 ± 1.67^{c}	20.27 ± 0.77^{c}	19.08 ± 0.31^{c}	23.01 ± 0.55^{c}	22.81 ± 0.22^{c}

The figures are the mean value ±standard deviation in the table.

a, b, c, d, e, means followed by different superscripts in the same column are significantly different at $p < 0.05$.

a, b, c, d, e, means followed by the same superscripts in the same column are not significantly different at $p > 0.05$.

HMF and furfurals were the intermediate products of degradation of cellulose, hemicellulose, and lignin during the HTC process. Their concentrations firstly increased and then decreased with the increase of PWR number (**Table 3**). The variation trend of HMF concentration was consistent with the changing of the mass yield of hydrochar (**Table 1**), indicating that HMF played a specific role in increasing the mass yield of hydrochar. It is shown that HMF could be polymerized into heavier compounds and deposited on the surface of hydrochar during the HTC PWR process, thus increasing the mass yield of hydrochar (Castello et al., 2015). HMF has various value-added applications in the chemical and biological regeneration industry (Kambo et al., 2018), and its recycling also has great utilization value. Therefore, there were some valuable products in the liquid by-products after HTC PWR, which could catalyze HTC to improve WS hydrochar. These products also could be recycled and applied to biochemical production.

3.2 Effects of Microwave Energy Activation on Temperature-rising Properties of Wheat Straw Hydrochar

Effects of different microwave power and microwave activation duration on temperature-rising properties of WS hydrochar are shown in **Figure 6**. With increasing microwave power or microwave activation duration, the temperature-rising properties of HTC-PWR2 hydrochar and HTC-PWR3 hydrochar significantly increased. Under the conditions of high microwave power and long microwave activation duration, changes in the temperature of hydrochar were not significantly obvious. Thus, in order to save energy and reduce consumption, the activation of hydrochar could be carried out under the condition of MEA1000-4. The temperature-rising properties of wheat straw hydrochar were significantly different under the conditions of various PWR (**Figures 6A,B**). The temperature-rising property of HTC-PWR2 hydrochar was much higher than that of HTC-PWR3 hydrochar.

3.3 Effects of Microwave Energy Activation on Fuel Properties of Wheat Straw Hydrochar

Effects of different microwave power and microwave activation duration on the mass and energy yields of WS hydrochar are listed in **Table 4**. With the increase of microwave power or the extension of microwave activation duration, the mass yield of hydrochar decreased. With increasing microwave power, the energy yield of HTC-PWR2 hydrochar decreased. With the extension of microwave activation duration, the energy yield firstly increased and then decreased. The energy yield (46.18%) of HTC-PWR2 hydrochar was the highest under the condition of MEA900-4. The energy yields of HTC-PWR2 hydrochar were

much higher than those of HTC-PWR3 hydrochar under the same condition of microwave power and microwave activation duration.

Effects of different microwave power and microwave activation duration on proximate analysis and HHV of WS hydrochar are listed in **Table 5**. The ash contents had significant differences under the various microwave conditions, which were lower in HTC-PWR2 hydrochar than those in HTC-PWR3 hydrochar. The ash content (2.69%) of HTC-PWR2 hydrochar was the lowest under the condition of MEA900-4. The volatile contents of hydrochar decreased and their fixed carbon contents and HHV increased with the increase of microwave power. The volatile content (70.19%) of HTC-PWR2 hydrochar was the lowest, its fixed carbon content (25.96%) and HHV (24.17 MJ/kg) were the highest under the condition of MEA1000-4. The proximate analysis and HHV between HTC-PWR2 hydrochar and HTC-PWR3 hydrochar were different under the same microwave conditions, indicating that different PWR numbers had effects on the properties of hydrochar modified by microwave. In conclusion, the fuel properties of hydrochar were improved after MEA.

4 CONCLUSION

The mass yield (58.25%) and energy yield (71.84%) of hydrochar were the highest under the condition of HTC-PWR3, which increased by 14.91% and 17.54% compared with that under the condition of HTC-PWR0, respectively. After HTC-PWR2, the carbon content (55.59%) and HHV (21.72 MJ/kg) were the highest, and the ash content (1.93%) was the lowest. After HTC-PWR3, the fixed carbon content (18.53%) was the highest. According to the analysis of O/C and H/C ratios, HTC-PWR2 hydrochar has the potential to become a high-value fuel. With the increase of PWR times, carbon microspheres firstly increased and then melted, and much more pores appeared on the surface of hydrochar, and the concentration of all organic acids increased, and the concentrations of HMF and furfurals firstly increased and then decreased, which were conducive to the rise of carbon content, the improvement of HHV, and the changing of mass yield.

With the increase of microwave power or the extension of microwave activation duration, the temperature-rising properties of hydrochar significantly increased. The energy yield (46.18%) and ash content (2.69%) of HTC-PWR2 hydrochar were the highest under the condition of MEA900-4. The volatile content (70.19%) of HTC-PWR2 hydrochar was the lowest, its fixed carbon content (25.96%) and HHV (24.17 MJ/kg) were the highest under the condition of MEA1000-4, which were higher than those of hydrochar only treated by HTC PWR.

Different MEA conditions had modified effects on the properties of hydrochar after HTC PWR. The HTC PWR and MEA had synergistic effects on improving properties of WS. The properties of WS could be improved when WS was treated by the condition of HTC-PWR2 and activated under the condition of MEA900-4 or MEA1000-4.

DATA AVAILABILITY STATEMENT

The original contributions presented in the study are included in the article/Supplementary Material, further inquiries can be directed to the corresponding authors.

AUTHOR CONTRIBUTIONS

XZ: Investigation, Conceptualization, Methodology, Writing-original draft, Experimental analysis, drawing diagrams, Software, Data curation, Visualization, Editing, Funding acquisition; QQ: Investigation, Methodology, Experimental analysis, Data curation, drawing diagrams; XL: Conceptualization, Formal analysis; WW: Conceptualization, Supervision, Funding acquisition, Formal analysis, Validation, Review, Project administration.

FUNDING

This work was supported by the National Natural Science Foundation of China (51976110), the Postdoctoral Innovation Project of Shandong Province (202101002), the Young Scholars Program of Shandong University (2018WLJH75) and Natural Science Foundation of Shandong Province (ZR2019MEE035).

REFERENCES

Ao, W., Fu, J., Mao, X., Kang, Q., Ran, C., Liu, Y., et al. (2018). Microwave Assisted Preparation of Activated Carbon from Biomass: a Review. *Renew. Sust. Energ. Rev.* 92, 958–979. doi:10.1016/j.rser.2018.04.051

Castello, D., Kruse, A., and Fiori, L. (2015). Low Temperature Supercritical Water Gasification of Biomass Constituents: Glucose/phenol Mixtures. *Biomass and Bioenergy* 73, 84–94. doi:10.1016/j.biombioe.2014.12.010

Channiwala, S. A., and Parikh, P. P. (2002). A Unified Correlation for Estimating HHV of Solid, Liquid and Gaseous Fuels. *Fuel* 81, 1051–1063. doi:10.1016/S0016-2361(01)00131-4

Cui, Y. F., Jun, M., Wang, Q. X., Zhang, W. M., Cheng, X. Y., and Chen, W. F. (2018). Effects of Straw and Biochar Addition on Soil Nitrogen, Carbon, and Super rice Yield in Cold Waterlogged Paddy Soils of North China. *J. Integr. Agric.* 16, 1064–1074. doi:10.1016/S2095-3119(16)61578-2

de Caprariis, B., Scarsella, M., Bavasso, I., Bracciale, M. P., Tai, L., and De Filippis, P. (2021). Effect of Ni, Zn and Fe on Hydrothermal Liquefaction of Cellulose: Impact on Bio-Crude Yield and Composition. *J. Anal. Appl. Pyrolysis* 157, 105225. doi:10.1016/j.jaap.2021.105225

Funke, A., and Ziegler, F. (2010). Hydrothermal Carbonization of Biomass: a Summary and Discussion of Chemical Mechanisms for Process Engineering. *Biofuels, Bioprod. Bioref.* 4, 160–177. doi:10.1002/bbb.198

Ghaziaskar, A., McRae, G. A., Mackintosh, A., and Basu, O. D. (2019). Catalyzed Hydrothermal Carbonization with Process Liquid Recycling. *Energy Fuels* 33, 1167–1174. doi:10.1021/acs.energyfuels.8b03454

Heidari, M., Salaudeen, S., Dutta, A., and Acharya, B. (2018). Effects of Process Water Recycling and Particle Sizes on Hydrothermal Carbonization of Biomass. *Energy Fuels* 32, 11576–11586. doi:10.1021/acs.energyfuels.8b02684

Hu, Y., Sun, B., Wu, S., Feng, H., Gao, M., Zhang, B., et al. (2021). After-effects of Straw and Straw-Derived Biochar Application on Crop Growth, Yield, and Soil Properties in Wheat (*Triticum aestivum* L.) -maize (Zea mays L.) Rotations: A

Four-Year Field experiment. *Sci. Total Environ.* 780, 146560. doi:10.1016/j.scitotenv.2021.146560

Ibbett, R., Gaddipati, S., Davies, S., Hill, S., and Tucker, G. (2011). The Mechanisms of Hydrothermal Deconstruction of Lignocellulose: New Insights from thermal-analytical and Complementary Studies. *Bioresour. Tech.* 102, 9272–9278. doi:10.1016/j.biortech.2011.06.044

Jin, F., Zhou, Z., Moriya, T., Kishida, H., Higashijima, H., and Enomoto, H. (2005). Controlling Hydrothermal Reaction Pathways to Improve Acetic Acid Production from Carbohydrate Biomass. *Environ. Sci. Technol.* 39, 1893–1902. doi:10.1021/es048867a

Kabadayi Catalkopru, A., Kantarli, I. C., and Yanik, J. (2017). Effects of Spent Liquor Recirculation in Hydrothermal Carbonization. *Bioresour. Tech.* 226, 89–93. doi:10.1016/j.biortech.2016.12.015

Kaliyan, N., and Morey, R. V. (2010). Natural Binders and Solid Bridge Type Binding Mechanisms in Briquettes and Pellets Made from Corn stover and Switchgrass. *Bioresour. Tech.* 101, 1082–1090. doi:10.1016/j.biortech.2009.08.064

Kambo, H. S. (2014). *Energy Densification of Lignocellulosic Biomass via Hydrothermal Carbonization and Torrefaction*. [dissertation thesis]. Canada: University of Guelph.

Kambo, H. S., Minaret, J., and Dutta, A. (2018). Process Water from the Hydrothermal Carbonization of Biomass: a Waste or a Valuable Product? *Waste Biomass Valor.* 9, 1181–1189. doi:10.1007/s12649-017-9914-0

Knežević, D., van Swaaij, W. P. M., and Kersten, S. R. A. (2009). Hydrothermal Conversion of Biomass: I, Glucose Conversion in Hot Compressed Water. *Ind. Eng. Chem. Res.* 48, 4731–4743. doi:10.1021/ie801387v

Köchermann, J., Görsch, K., Wirth, B., Mühlenberg, J., and Klemm, M. (2018). Hydrothermal Carbonization: Temperature Influence on Hydrochar and Aqueous Phase Composition during Process Water Recirculation. *J. Environ. Chem. Eng.* 6, 5481–5487. doi:10.1016/j.jece.2018.07.053

Leng, L., Yang, L., Chen, J., Leng, S., Li, H., Li, H., et al. (2020). A Review on Pyrolysis of Protein-Rich Biomass: Nitrogen Transformation. *Bioresour. Tech.* 315, 123801. doi:10.1016/j.biortech.2020.123801

Leng, S., Leng, L., Chen, L., Chen, J., Chen, J., and Zhou, W. (2020). The Effect of Aqueous Phase Recirculation on Hydrothermal Liquefaction/carbonization of Biomass: A Review. *Bioresour. Tech.* 318, 124081. doi:10.1016/j.biortech.2020.124081

Li, Y., Liu, X., Zhang, P., Wang, X., Cao, Y., and Han, L. (2018). Qualitative and Quantitative Correlation of Physicochemical Characteristics and lead Sorption Behaviors of Crop Residue-Derived Chars. *Bioresour. Tech.* 270, 545–553. doi:10.1016/j.biortech.2018.09.078

Libra, J. A., Ro, K. S., Kammann, C., Funke, A., Berge, N. D., Neubauer, Y., et al. (2014). Hydrothermal Carbonization of Biomass Residuals: a Comparative Review of the Chemistry, Processes and Applications of Wet and Dry Pyrolysis. *Biofuels* 2, 71–106. doi:10.4155/bfs.10.81

Liu, Z., Quek, A., Kent Hoekman, S., and Balasubramanian, R. (2013). Production of Solid Biochar Fuel from Waste Biomass by Hydrothermal Carbonization. *Fuel* 103, 943–949. doi:10.1016/j.fuel.2012.07.069

Liu, X., Wu, Z., Han, Y., and Han, L. (2017). Characteristic Modification of Alkalized Corn Stalk and Contribution to the Bonding Mechanism of Fuel Briquette. *Energy* 133, 299–305. doi:10.1016/j.energy.2017.05.083

Ma, Q., Han, L., and Huang, G. (2018). Effect of Water-Washing of Wheat Straw and Hydrothermal Temperature on its Hydrochar Evolution and Combustion Properties. *Bioresour. Tech.* 269, 96–103. doi:10.1016/j.biortech.2018.08.082

Ma, L., Kong, F., Wang, Z., Luo, Y., Lv, X., Zhou, Z., et al. (2019). Growth and Yield of Cotton as Affected by Different Straw Returning Modes with an Equivalent Carbon Input. *Field Crops Res.* 243, 107616. doi:10.1016/j.fcr.2019.107616

Poddar, S., Kamruzzaman, M., Sujan, S. M. A., Hossain, M., Jamal, M. S., Gafur, M. A., et al. (2014). Effect of Compression Pressure on Lignocellulosic Biomass Pellet to Improve Fuel Properties: Higher Heating Value. *Fuel* 131, 43–48. doi:10.1016/j.fuel.2014.04.061

Reza, M. T. (2011). *Hydrothermal Carbonization of Lignocellulosic Biomass*. [dissertation thesis]. Reno: University of Nevada.

Reza, M. T., Lynam, J. G., Uddin, M. H., and Coronella, C. J. (2013). Hydrothermal Carbonization: Fate of Inorganics. *Biomass and Bioenergy* 49, 86–94. doi:10.1016/j.biombioe.2012.12.004

Salak Asghari, F., and Yoshida, H. (2006). Acid-catalyzed Production of 5-hydroxymethyl Furfural from D-Fructose in Subcritical Water. *Ind. Eng. Chem. Res.* 45 (7), 2163–2173. doi:10.1021/ie051088y

Sluiter, A., Hames, B., Ruiz, R., Scarlata, C., Sluiter, J., and Templeton, D. (2006). *Determination of Sugars, Byproducts, and Degradation Products in Liquid Fraction Process Samples*. Washington, DC: NREL National Renewable Energy Laboratory, Office of Energy Efficiency and Renewable Energy, U.S. Department of Energy. NREL/TP-510-42623.

Stemann, J., Erlach, B., and Ziegler, F. (2013a). Hydrothermal Carbonisation of Empty palm Oil Fruit Bunches: Laboratory Trials, Plant Simulation, Carbon Avoidance, and Economic Feasibility. *Waste Biomass Valor.* 4, 441–454. doi:10.1007/s12649-012-9190-y

Stemann, J., Putschew, A., and Ziegler, F. (2013b). Hydrothermal Carbonization: Process Water Characterization and Effects of Water Recirculation. *Bioresour. Tech.* 143, 139–146. doi:10.1016/j.biortech.2013.05.098

Tai, L., de Caprariis, B., Scarsella, M., De Filippis, P., and Marra, F. (2021). Improved Quality Bio-Crude from Hydrothermal Liquefaction of Oak wood Assisted by Zero-Valent Metals. *Energy Fuels* 35, 10023–10034. doi:10.1021/acs.energyfuels.1c00889

Telmo, C., Lousada, J., and Moreira, N. (2010). Proximate Analysis, Backwards Stepwise Regression between Gross Calorific Value, Ultimate and Chemical Analysis of wood. *Bioresour. Tech.* 101, 3808–3815. doi:10.1016/j.biortech.2010.04.00910.1016/j.biortech.2010.01.021

Titirici, M.-M., and Antonietti, M. (2010). Chemistry and Materials Options of Sustainable Carbon Materials Made by Hydrothermal Carbonization. *Chem. Soc. Rev.* 39, 103–116. doi:10.1039/B819318P

Uddin, M. H., Reza, M. T., Lynam, J. G., and Coronella, C. J. (2013). Effects of Water Recycling in Hydrothermal Carbonization of Loblolly pine. *Environ. Prog. Sust. Energ.* 33, a–n. doi:10.1002/ep.11899

Wang, F., Wang, J., Gu, C., Han, Y., Zan, S., and Wu, S. (2019). Effects of Process Water Recirculation on Solid and Liquid Products from Hydrothermal Carbonization of Laminaria. *Bioresour. Tech.* 292, 121996. doi:10.1016/j.biortech.2019.121996

Weiner, B., Poerschmann, J., Wedwitschka, H., Koehler, R., and Kopinke, F.-D. (2014). Influence of Process Water Reuse on the Hydrothermal Carbonization of Paper. *ACS Sust. Chem. Eng.* 2, 2165–2171. doi:10.1021/sc500348v

Wirth, B., and Mumme, J. (2013). Anaerobic Digestion of Waste Water From Hydrothermal Carbonization of Corn Silage. *Appl. Energy*, 1–10. doi:10.2478/apbi-2013-0001

Zhang, B., and Zhang, J. (2017). Influence of Reaction Atmosphere (N2, CO, CO2, and H2) on ZSM-5 Catalyzed Microwave-Induced Fast Pyrolysis of Medicinal Herb Residue for Biofuel Production. *Energy Fuels* 31, 9627–9632. doi:10.1021/acs.energyfuels.7b02106

Zhang, X., Han, L., Peng, W., Xiao, W., and Liu, X. (2018). Effects of Different Pretreatments on Compression Molding of Wheat Straw and Mechanism Analysis. *Bioresour. Tech.* 251, 210–217. doi:10.1016/j.biortech.2017.12.015

Zhang, X., Li, Y., Wang, M., Han, L., and Liu, X. (2019). Effects of Hydrothermal Carbonization Conditions on the Combustion and Kinetics of Wheat Straw Hydrochar Pellets and Efficiency Improvement Analyses. *Energy Fuels* 34, 587–598. doi:10.1021/acs.energyfuels.9b03754

Zhang, X., Zhao, S., Gao, B., Wu, P., Han, L., and Liu, X. (2020). Optimization of a "Coal-like" Pelletization Technique Based on the Sustainable Biomass Fuel of Hydrothermal Carbonization of Wheat Straw. *J. Clean. Prod.* 242, 118426. doi:10.1016/j.jclepro.2019.118426

Zhou, Y., Yan, W., Yu, X., Chen, T., Wang, S., and Zhao, W. (2020). Boron and Nitrogen Co-doped Porous Carbon for Supercapacitors: A Comparison between a Microwave-Assisted and a Conventional Hydrothermal Process. *J. Energ. Storage* 32, 101706. doi:10.1016/j.est.2020.101706

Zhu, Z., Toor, S. S., Rosendahl, L., Yu, D., and Chen, G. (2015). Influence of Alkali Catalyst on Product Yield and Properties via Hydrothermal Liquefaction of Barley Straw. *Energy* 80, 284–292. doi:10.1016/j.energy.2014.11.071

Zhu, G., Yang, L., Gao, Y., Xu, J., Chen, H., Zhu, Y., et al. (2019). Characterization and Pelletization of Cotton Stalk Hydrochar from HTC and Combustion Kinetics of Hydrochar Pellets by TGA. *Fuel* 244, 479–491. doi:10.1016/j.fuel.2019.02.039

Conflict of Interest: The authors declare that the research was conducted in the absence of any commercial or financial relationships that could be construed as a potential conflict of interest.

Publisher's Note: All claims expressed in this article are solely those of the authors and do not necessarily represent those of their affiliated organizations, or those of the publisher, the editors and the reviewers. Any product that may be evaluated in this article, or claim that may be made by its manufacturer, is not guaranteed or endorsed by the publisher.